

## Article

# Impacts of High-Concentration Turbid Water on the Groundwater Environment of the Tedor River Alluvial Fan in Japan

Yoichi Fujihara <sup>1,\*</sup> , Kento Otani <sup>2</sup>, Keiji Takase <sup>1</sup>, Shunsuke Chono <sup>1</sup> and Eiji Ichion <sup>1</sup>

<sup>1</sup> Faculty of Bioresources and Environmental Sciences, Ishikawa Prefectural University, Nonoichi 921-8836, Japan; hytakase@gmail.com (K.T.); chono@ishikawa-pu.ac.jp (S.C.); ichion@ishikawa-pu.ac.jp (E.I.)

<sup>2</sup> Kokusai Kogyo Co., Ltd., 2-24-1 Harumi-cho, Fuchu, Tokyo 183-0057, Japan; kento\_otani@kk-grp.jp

\* Correspondence: yfujii@ishikawa-pu.ac.jp; Tel.: +81-76-227-7479

**Abstract:** The occurrence of high-concentration turbid water due to a large landslide in the upper reaches of the Tedor River Basin in Japan in May 2015 led to a rapid decline in the groundwater levels within the alluvial fan. However, factors other than turbid water, such as changes in precipitation patterns, can have a significant impact on groundwater levels but have not been thoroughly investigated. By analyzing the relationship between river water and groundwater levels, we found that by 2018, conditions had returned to those observed prior to the turbidity events. Regarding seepage, we found that approximately 24% of the Tedor River's discharge contributed to seepage before the turbidity event. In contrast, during the post-turbidity years, seepage decreased between 2015 and 2017 and returned to the pre-turbidity levels by 2018. Furthermore, by constructing a hydrological model and examining the contributions of turbidity and precipitation, we found that in 2015, turbidity contributed to 76% of the groundwater level changes, whereas precipitation accounted for 24%. In contrast, in 2016, turbidity contributed to 67%, while precipitation contributed to 33%. In essence, the first year was characterized by a significant contribution from turbidity, while precipitation also played a significant role in groundwater level fluctuations in the second year.

**Keywords:** groundwater; alluvial fan; landslide; turbid water; seepage from river



**Citation:** Fujihara, Y.; Otani, K.; Takase, K.; Chono, S.; Ichion, E. Impacts of High-Concentration Turbid Water on the Groundwater Environment of the Tedor River Alluvial Fan in Japan. *Water* **2024**, *16*, 1326. <https://doi.org/10.3390/w16101326>

Academic Editor:  
Aristotelis Mantoglou

Received: 10 April 2024  
Revised: 30 April 2024  
Accepted: 2 May 2024  
Published: 7 May 2024



**Copyright:** © 2024 by the authors. Licensee MDPI, Basel, Switzerland. This article is an open access article distributed under the terms and conditions of the Creative Commons Attribution (CC BY) license (<https://creativecommons.org/licenses/by/4.0/>).

## 1. Introduction

Annual groundwater usage in Japan is approximately 8.6 billion m<sup>3</sup>/year, accounting for 11% of the total water usage, which is approximately 78.5 billion m<sup>3</sup>/year [1]. The region with the highest dependence on groundwater for urban use (domestic and industrial usage) is the Hokuriku region, located on the Sea of Japan's side of Japan, where the groundwater dependency rate is approximately 48% [1]. In this region, groundwater resources are abundant in terrains characterized by substantial thickness and high porosity, such as alluvial fans and plains [2]. In these areas, paddy fields are widespread and river water is usually diverted at the apexes of alluvial fans and delivered through a network of irrigation canals to each paddy field. Seepage from rivers and paddy fields contributes considerably to groundwater recharge [3]. Therefore, a precise understanding of the water cycle processes in alluvial fans and plains is essential for effective groundwater management (e.g., Tsuchihara et al. [3]; Yu and Chu [4]).

There are several alluvial fans in the Hokuriku region of Japan; however, the alluvial fan extending downstream from the Tedor River Basin in Ishikawa Prefecture (Figure 1) is a rich source for research. For instance, studies related to the Tedor River Basin include those by Noto et al. [5,6], who attempted to estimate the amount of snow stored within the basin. Maruyama et al. [7] and Fujihara et al. [8] conducted comprehensive studies on the mechanisms of snow accumulation and snowmelt in this basin. Furthermore, concerning

the Tedorì River alluvial fan, Iwasaki et al. [9] and Yoshioka et al. [10,11] analyzed the characteristics of the groundwater within the alluvial fan, utilizing data on groundwater levels, water quality, stable isotopic ratios and so on. Maruyama et al. [12] provided insights into the water balance within alluvial fans, whereas Yoshioka et al. [13] employed a 3D groundwater flow model (MODFLOW) to simulate groundwater systems under climate change conditions. Consequently, due to the accumulation of scientific knowledge and data related to the Tedorì River Basin and alluvial fan, a significant understanding of the water cycle within the basin and alluvial fan has been achieved.

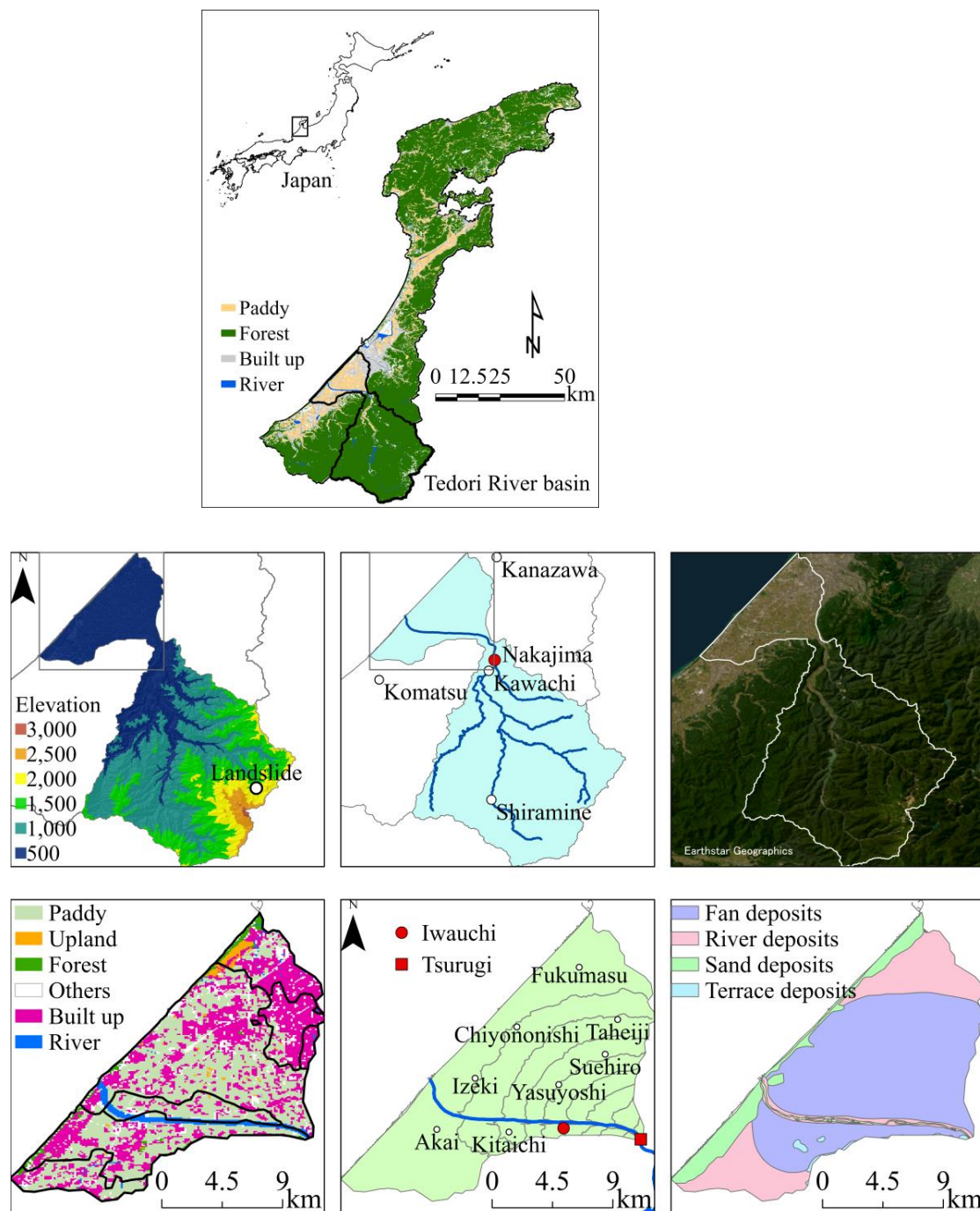


**Figure 1.** A map of Japan and Ishikawa Prefecture, and the location of the Tedorì River Basin and alluvial fan. The elevation, river channel, satellite image, land use, groundwater observation wells, and geology are also represented.

In May 2015, approximately 60 km upstream from the mouth of the Tedoru River, a large-scale landslide occurred in association with snowmelt. The scarp was approximately 400 m long and 300 m wide, with a maximum depth of 45 m (Figure 2), resulting in an erosion volume of approximately 1.3 million m<sup>3</sup> [14]. Following this landslide event, a high concentration of turbid water was observed downstream from the Tedoru River and in the agricultural water channels within the alluvial fan, and a rapid decline in groundwater levels within the alluvial fan occurred [15,16]. Furthermore, the reduction in groundwater levels led to the disappearance of and decrease in spring water, significantly impacting the habitats of endangered species, such as the freshwater-type nine-spined stickleback [17].

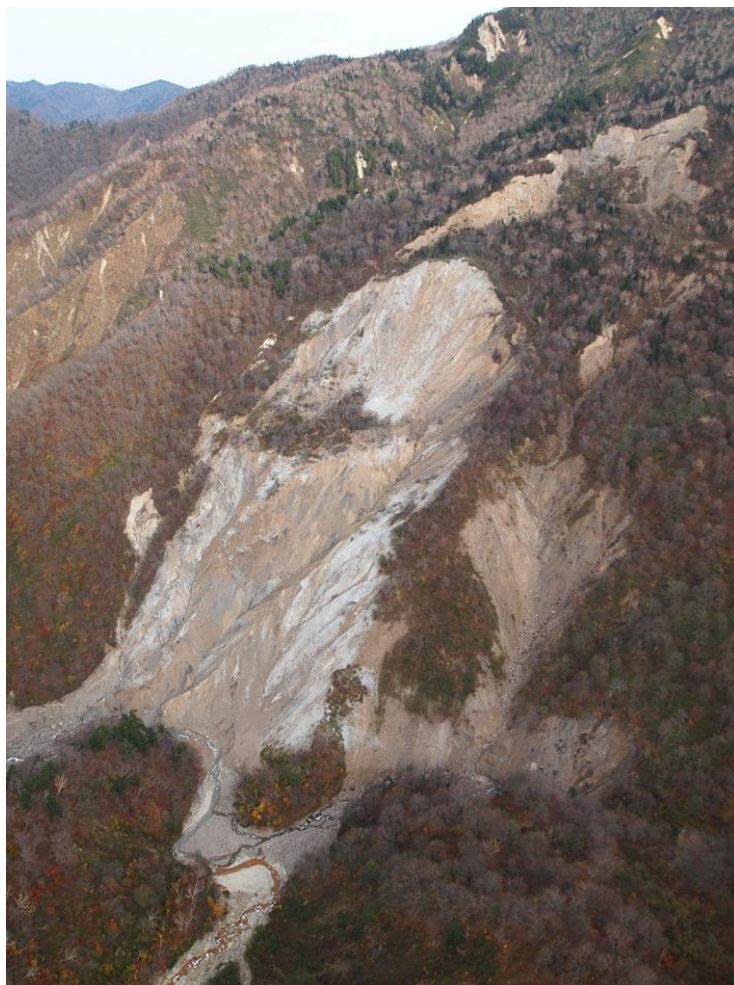


**Figure 2.** Photograph of the large-scale landslide. (photograph: by Prof. Seiji Yanai, date: 27 October 2015).

Tanaka et al. [15,16] investigated the infiltration rates in paddy fields and rivers and reported a potential reduction in these infiltration rates. Furthermore, Yoshioka et al. [18,19] reported possible changes in the exchange of river water with groundwater and alterations in groundwater recharge sources using the oxygen and hydrogen isotopic ratios of groundwater. However, these studies were based on infrequent on-site observations, typically conducted twice a year, resulting in fragmented results. Consequently, the duration of groundwater level decline and the time required for it to return to its normal state have not been adequately explored. Additionally, factors other than turbid water, such as changes in precipitation patterns, can have a significant impact on groundwater levels but have not been thoroughly investigated thus far. A more detailed understanding of the groundwater recovery processes and the contribution of each factor is needed for future the conservation and management of groundwater.



Therefore, in this study, we attempted to elucidate the decline and recovery processes of groundwater recharge within the Tedor River alluvial fan by analyzing continuously monitored groundwater levels and measuring river seepage. Additionally, we utilized a hydrological model to investigate the extent to which factors other than turbid water contribute to the decline in groundwater levels.

## 2. Study Area

### 2.1. Hydrogeology

The Tedor River, which originates from Mt. Hakusan at an elevation of 2702 m, has a length of 72 km and features a gradient of approximately 1/27, making it one of Japan's steepest rivers (Figure 1). The basin covers an area of 809 km<sup>2</sup>, and approximately 90% of the basin consists of mountainous terrain. However, in the downstream region, a typical alluvial fan has formed. The Tedor River alluvial fan, centered around Tsurugi in Hakusan City, Ishikawa Prefecture, has a radius of approximately 13 km and an opening angle of 110°. Its northeastern boundary is defined by the Fushimi River, and its southern boundary is marked by the Kakehashi River, encompassing an area of approximately 17,000 ha. The elevation at the fan's apex is approximately 80 m and exhibits an average gradient of approximately 1/150, featuring the characteristic steep topography of the Hokuriku region.

The Tedor River watershed experiences a climate unique to the Sea of Japan's side of the island, with an annual precipitation of approximately 2500 mm in Kanazawa. In mountainous areas, the annual precipitation reaches approximately 4000 mm due to winter snowfall [5]. Owing to this abundant water resource, the Tedor River alluvial fan has become a hub for various industries, including agriculture, industry, and commerce, making it the central region of Ishikawa Prefecture. Surface water is primarily utilized for irrigation purposes and is sourced from Hakusan headworks, providing water to approximately 8000 ha of paddy fields through the Shichika and Miyatake irrigation canals on the right and left banks, respectively. Groundwater resources are used by industries, such as sake brewing, textile production, and advanced manufacturing, contributing to regional development [5].

According to the Hokuriku Regional Agricultural Administration Office [20], the fan primarily consists of sandy gravel with a maximum thickness exceeding 130 m at its center. The shallow aquifer is composed of sandy gravel from the Quaternary period, whereas the deep aquifer consists of sandy gravel from the Quaternary or Paleogene-Neogene periods, occasionally containing some clay, and is underlain by bedrock from the Paleogene-Neogene era. In coastal areas, there is a layer of clay at depths of several tens of meters within a sandy gravel sequence [11]. Hydraulic conductivities, estimated through field and laboratory tests, range from 40 to 230 m/day for the shallow aquifer and 1.7 m/day for the deep aquifer, indicating relatively high permeability in both aquifer layers.

### 2.2. Landslide and Turbid Water Event

A landslide accompanied by snowmelt occurred in May 2015 in an area approximately 60 km upstream from the Tedor River (Figures 1 and 2). Subsequently, significantly turbid water was observed in the main stream of the Tedor River (Figure 3). In 2015, the average turbidity was 219 Nephelometric Turbidity Units (NTU), with a maximum value of 4012 NTU. In 2016, the average turbidity was 75 NTU, with a maximum value of 3363 NTU. In 2014, before the turbidity event, the average turbidity was only 18 NTU, with a maximum of 65 NTU, highlighting the extremely high turbidity levels after the turbidity event. Turbid water was drawn from the Tedor River at the apex of the fan and subsequently flowed through a network of irrigation channels, ultimately supplying water to paddy fields. Furthermore, sediment accumulation was observed at locations within the irrigation channels where the flow velocity slowed, often due to drop work and weirs [14].

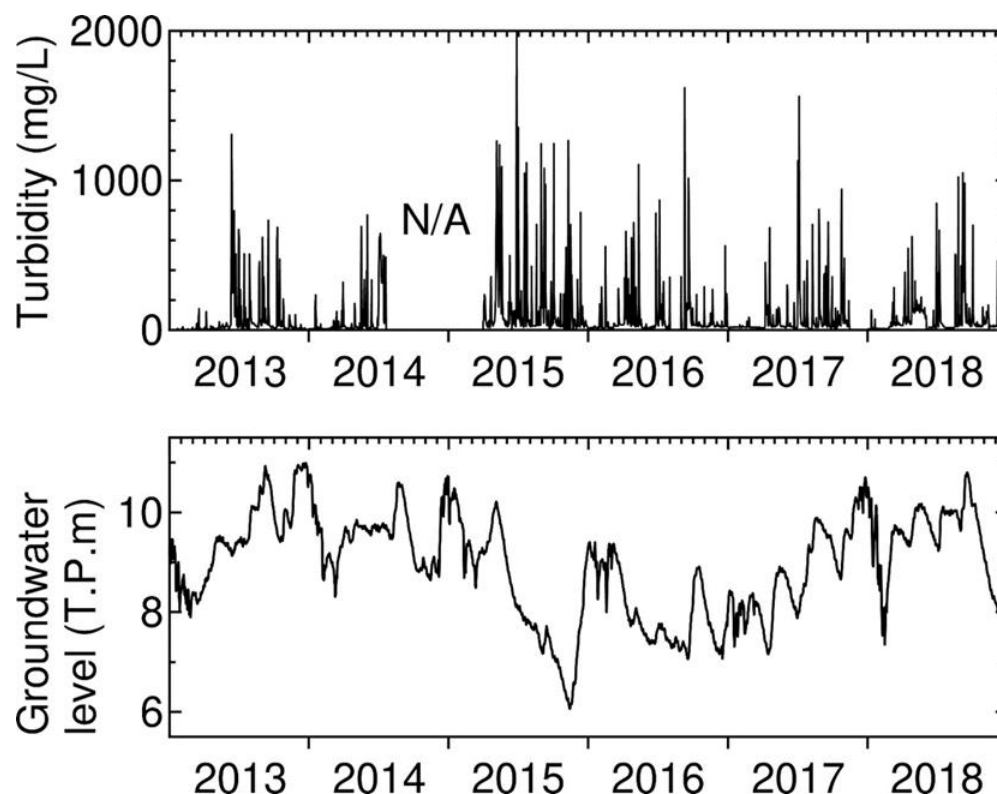


**Figure 3.** The time series data of turbidity at the main stream of the Tedor River and the average groundwater levels for the entire alluvial fan.

Ishikawa Prefecture maintains continuous groundwater monitoring within the fan, and data from groundwater level measurements at eight locations on both the right and left banks of the Tedor River (Kitaichi, Yasuyoshi, Suehiro, Taheiji, Akai, Izeiki, Chiyononishi, and Fukumasu) were examined. Although different trends were observed for each monitoring well, the weighted average groundwater levels were calculated using the Thiessen method. The weighted average groundwater levels revealed a significant decline in groundwater levels following the turbidity events in 2015 and 2016 (Figure 3). The average groundwater levels in 2013 and 2014, prior to the turbidity events, were 9.5 m. In contrast, the average groundwater level in 2015 dropped to 8.3 m, and in 2016, was further reduced to 8.0 m, demonstrating the rapid decline in groundwater levels after the turbidity events.

### 3. Methods

#### 3.1. Analysis of Relationships between River and Groundwater Levels

In general, in alluvial fans and plains, the ground is highly permeable, resulting in river water levels being higher than the surrounding groundwater levels. With the exception of the coastal area, the Tedor River alluvial fan behaves like a losing river. In other words, groundwater recharge originates from the river flow passing through the alluvial fan. Because the saturated percolation flow can be determined using Darcy's law, it is suggested that the difference between the observed river water levels and the groundwater levels at fixed observation points is proportional to the groundwater recharge. If turbid water upstream has accumulated fine-grained sand and clogs the riverbed pores (e.g., Goldschneider et al. [21]; Lamontagne et al. [22]; Dubuis and Cesare [23]), the recharge rate, that is, the relationship between the river water level and the groundwater level, is also likely to change. Furthermore, when clogging in riverbed pores is alleviated, the relationship between river water and groundwater levels is expected to return to its pre-turbid water state. Therefore, we aimed to continuously analyze the changes in recharge

by examining the relationship between river and groundwater levels at fixed observation points where water levels are monitored.

River flow measurements were conducted at the Nakajima station; however, agricultural water intake was carried out at the downstream headwork. Consequently, within the alluvial fan, the river flow downstream from this station was lower than that at the Nakajima station. Therefore, in this study, we analyzed the river water level at the Tsurugi point (Figure 1), where only the water level is monitored. Groundwater levels were widely observed within the alluvial fan. To investigate changes in the amount of seepage from the river, it is appropriate to use groundwater monitoring wells closer to the river. Therefore, we analyzed groundwater levels at the Iwauchi point (Figure 1). Both river water and groundwater level observations were conducted by the Ministry of Land, Infrastructure, Transport, and Tourism, and data from a ten-year period between 2009 and 2018 were obtained for analysis.

### 3.2. Measurement of River Seepage

To elucidate the water balance structure in the fan, Maruyama et al. [12] conducted seepage surveys in 2009 prior to the turbidity event. In our study, multiple observations similar to those of Maruyama et al. [12] were conducted to examine the changes in seepage from the river after the turbidity event. The target section for river flow observations extended from 1.1 km downstream from the Tedoru River mouth to 16.4 km upstream, encompassing the fan area (Figure 4). Flow observations were conducted at eight cross-sections along the main stream of the Tedoru River and 16 cross-sections at the tributaries and inflow points. In cases where river flow division occurred at the mainstream cross-sections, flow observations were conducted at multiple nearby cross-sections. The spacing between the measurement points for the water depths and flow velocities was set at 2 m for river widths less than 40 m and 4 m for river widths exceeding 40 m. In the vertical direction of flow velocity measurement, a single-point method was employed, with measurements taken at 60% of the water depth for water depths less than 0.75 m, and a two-point method at 20% and 80% of the water depth for depths exceeding 0.75 m. All observations were conducted within a single day to minimize water balance errors in flow measurements. Water balance calculations (e.g., Harte and Kiah [24]; Kinzli et al. [25]; Martin and Gates [26]) were performed using the flow observation results at the main stream, tributaries, and inlets, and the increment/decrease for each section in the main stream was obtained. A positive value for the sectional increase/decrease indicates an upwelling section that flows into the river from the groundwater, whereas a negative value indicates a losing section that infiltrates groundwater from the river.

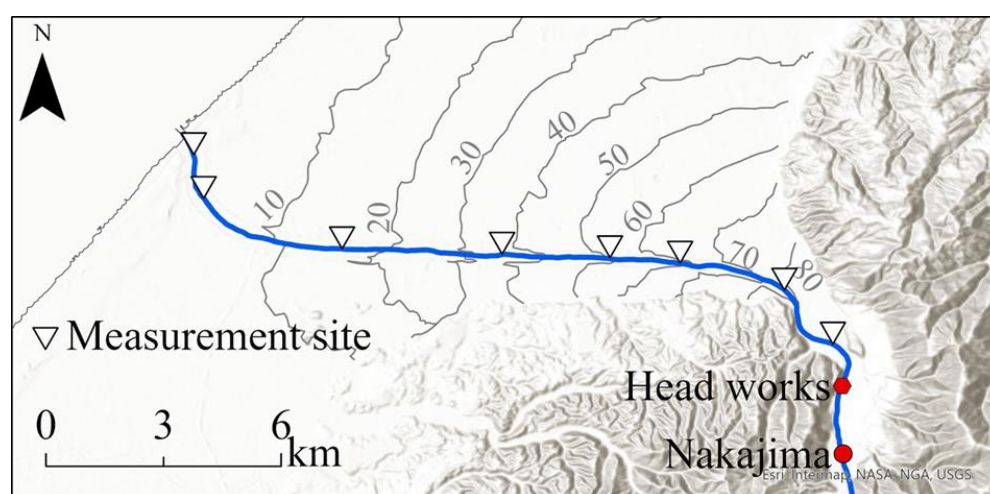


**Figure 4.** Location of river flow measurement points. River flow is continuously observed at Nakajima point and irrigation water is taken at the headworks.

Given the presence of errors in river flow measurements, it is advantageous to have a substantial number of observations when investigating changes in seepage before and after turbidity events. As mentioned in the Introduction and the Study area sections, one notable feature of the Tedor River fan area is the substantial amount of past research efforts regarding it. Moreover, the Ministry of Land, Infrastructure, Transport, and Tourism conducted simultaneous river flow observations, and the results were compiled by Yoshioka et al. [18]. While it cannot be definitively stated that the Ministry of Land, Infrastructure, Transport, and Tourism employed methods identical to those of our study, the number of river cross-sections surveyed was nearly the same. Therefore, we incorporated observations from the Ministry of Land, Infrastructure, Transport, and Tourism into our analysis. A summary of the observational data used to estimate the groundwater recharge is presented in Table 1. As a result, we obtained 12 data points from before the turbidity event and 6 data points after the turbidity event.

**Table 1.** List of flow observations.

Before the occurrence of turbidity		
Observation year	Month-day	Observer
2003	August-7, October-7	MLIT
2004	August-22, August-29	MLIT
2005	February-13, October-2	MLIT
2009	June-4, December-2	ISPU
	October-22	MLIT
2010	August-29	MLIT
2013	January-13	MLIT
2014	October-10	MLIT
After the occurrence of turbidity		
Observation year	Month-day	Observer
2015	June-25, August-15	MLIT
2016	June-8, December-12	ISPU
2017	June-23	ISPU
2018	June-19	ISPU

Note: MLIT: Ministry of Land, Infrastructure, Transport, and Tourism. ISPU: Ishikawa Prefectural University.

### 3.3. Hydrological Model for Contribution Estimation

Based on previous research (Tanaka et al. [15,16]; Yoshioka et al. [18,19]), the primary factor leading to the decline in groundwater levels is the reduction in recharge due to the clogging caused by turbid water. However, precipitation also has a significant impact on groundwater fluctuations. To analyze these complex factors, it is considered effective to conduct a scenario analysis using a hydrological model that represents the water circulation within the alluvial fan. It is generally believed that the spatial distribution of geology and soil properties has a significant influence on hydrological characteristics [27], and 3D groundwater models are often employed for impact assessment (e.g., Thakur [28]; Siena and Riva [29]). However, the Tedor River alluvial fan is composed of relatively uniform sandy gravel deposits.

Therefore, we constructed a hydrological model (Figure 5) to represent the water circulation within the entire alluvial fan in three distinct zones: the surface, intermediate, and groundwater levels. The input elements into the surface zone included precipitation and irrigation water from the upper reaches of the Tedor River. Conversely, the output elements from the surface zone included evapotranspiration, surface runoff from rain and snow accumulation and melt within the alluvial fan, and infiltration from paddy fields and other land uses into the intermediate zone. Within the intermediate zone, the input elements consisted of subsurface flow from the Tedor River and infiltration from the surface zone, whereas the output elements encompassed the intermediate outflow to the sea and infiltration into the groundwater zone. The input to the groundwater zone

is represented solely by infiltration from the intermediate zone, and the output elements include outflows to the sea and groundwater pumped for urban water supply purposes. In this model, variations in the storage depth of the groundwater zone represent typical fluctuations in the groundwater levels within the alluvial fan. Further details on this model can be found in Takase and Fuhara [30,31].

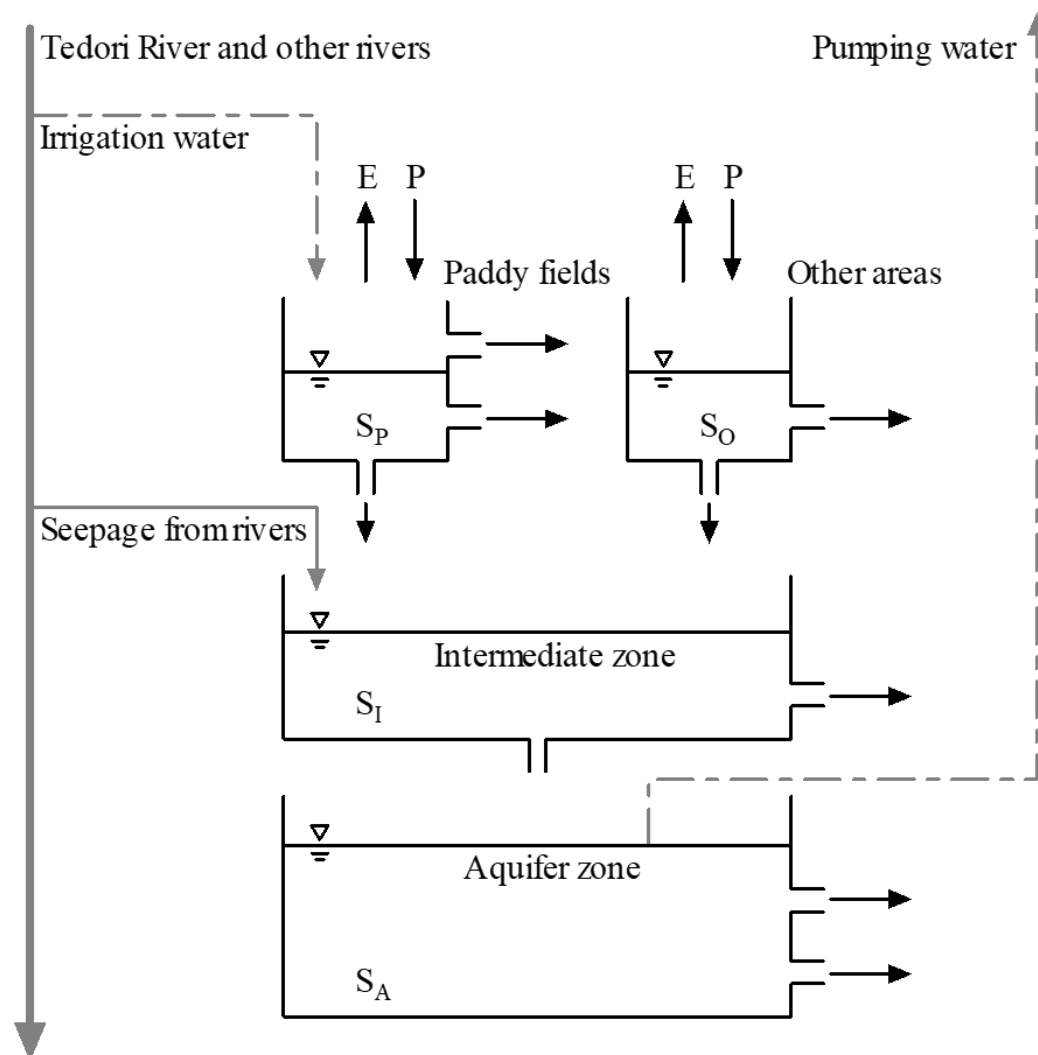


**Figure 5.** Structure of the hydrological model used in this study.

The groundwater level data used for model analysis were obtained from eight locations situated on the right and left banks of the Tedori River, as described above in Section 2.1. These locations included Kitaichi, Yasuyoshi, Suehiro, Taheiji, Akai, Izeki, Chiyononishi, and Fukumasu (Figure 1). The daily groundwater levels from these locations were weighted according to their respective areas using the Thiessen method. Daily precipitation data were derived from the average values recorded at the Kanazawa Local Meteorological Office and the Komatsu Automated Meteorological Data Acquisition System (AMeDAS) station and served as input data for the model. Daily evapotranspiration was calculated using the Penman equation based on meteorological data from the Kanazawa Local Meteorological Office, and this value was used as input data for the model. The inflow from the upper reaches of the Tedori River was determined using actual daily flow data observed at the Nakajima station. These flow measurements were continuously monitored by the Ministry of Land, Infrastructure, Transport, and Tourism. The analysis period spanned six years, from 2013 to 2018, during which data were available and collected for analysis.



The parameters included in the hydrological model encompassed those related to the outflow and infiltration from each tank zone, the infiltration from the Tadori River, and the parameters associated with snowfall and snowmelt. Physically determined parameters, such as effective porosity, were determined by referencing past research findings. Conversely, parameters that could not be directly determined were established using an Evolution Strategy, which is a global optimization method (Fujihara et al. [32]; Hang and Chikamori [33]). The Evolution Strategy has been reported to possess capabilities equivalent to those of the SCE-UA method (Duan et al. [34,35]) despite its relative simplicity. In this study, we calibrated the model parameters using data from the pre-turbid water period from 2013 to 2014. Model performance was evaluated using the Nash–Sutcliffe efficiency (NSE), relative error (RE), and percent bias (PBIAS), following Gupta et al. [36], De Vos et al. [37], and Shi et al. [38].

$$NSE = 1 - \Sigma(Ho,i - Hc,i)^2 / \Sigma(Ho,i - Hmean)^2 \quad (1)$$

$$RE = 1/N \Sigma |Ho,i - Hc,i| / Ho,I \times 100 \quad (2)$$

$$PBIAS = \Sigma(Ho,i - Hc,i) / \Sigma Ho,I \times 100 \quad (3)$$

where  $Ho,i$  is the observed daily groundwater level,  $Hc,i$  is the calculated daily groundwater level,  $Hmean$  is the mean groundwater level,  $i$  is the time, and  $N$  is the number of data points.

### 3.4. Contribution Estimation

By establishing a model that accurately reproduces groundwater levels during the calibration period before the turbidity events (2013–2014), we simulated the groundwater environment in the absence of turbidity effects. Since the amount of groundwater use did not change significantly during the analysis period, the difference between the modeled groundwater levels and the observed groundwater levels from 2015 onwards can be attributed to the impact of the turbidity events. Furthermore, it has been reported that the precipitation in the period of significant turbidity (2015 and 2016) was lower than usual (e.g., Yoshioka et al. [19]). This reduction in precipitation may have contributed to the decline in groundwater levels. To address this, the precipitation before and after the turbidity can be analyzed, and a scenario in which precipitation is as usual can be set up to simulate groundwater levels. Although there are sophisticated analysis methods using the Monte Carlo framework [39], in this study, the contributions of turbidity and precipitation were calculated using the following formulae, incorporating cases without turbidity effects and cases with neither turbidity effects nor normal precipitation levels:

$$\text{Turbidity Contribution} = 1/N \Sigma (Hcase(a),i - Ho,i) / (Hcase(b),i - Ho,i) \times 100 \quad (4)$$

$$\text{Precipitation Contribution} = 1/N \Sigma (Hcase(b),i - Hcase(a),i) / (Hcase(b),i - Ho,i) \times 100 \quad (5)$$

where  $Ho,i$  is the observed groundwater level,  $Hcase(a),i$  is the groundwater level in the absence of turbidity effects,  $Hcase(b),i$  is the groundwater level in the absence of turbidity effects with normal precipitation levels, and  $N$  is the number of data points considered in the calculations.

## 4. Results

### 4.1. Relationship between River and Groundwater Levels

Preliminary investigations on the relationship between river water levels (Tsurugi) and groundwater levels (Iwauchi) revealed a strong correlation between the 14-day backward moving average of river water and the groundwater levels. Therefore, in the following analysis, we utilized the 14-day backward moving average of river water level data. Figure 6 presents the time series of groundwater, river water, and the 14-day backward moving average of the river water levels. Although there are variations in the river water levels from year to year, the water levels tend to rise starting from early spring, when snowmelt commences in the upstream area. Additionally, water level spikes were observed from July

to September, which were mainly attributed to heavy rainfall events. In the Tedor River Basin, winter precipitation is abundant, but it accumulates as snowpack rather than leading to significant increases in river water levels. Groundwater levels tend to be lower during the winter months, when river water levels are also low. Conversely, groundwater levels increase in response to increases in river water levels caused by rainfall. This observation indicates a general alignment between fluctuations in river water and groundwater levels, where both tend to rise and fall together.

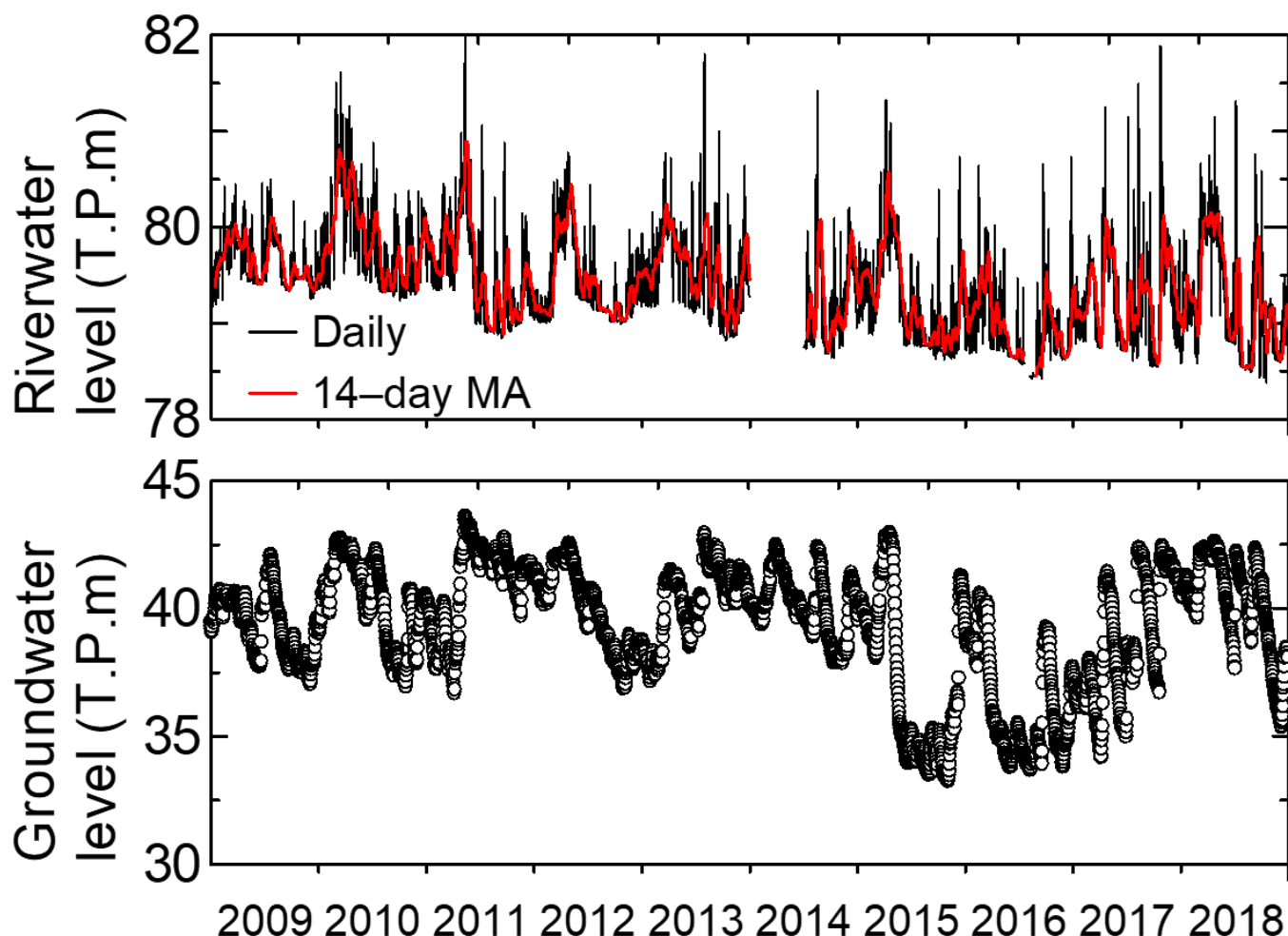


**Figure 6.** Time series data of river water, the 14-day backward moving average of river water, and groundwater levels.

To gain a more detailed understanding of the relationship between river water levels and groundwater levels, scatterplots of the river water levels and groundwater levels for each year are presented in Figure 7. As turbidity occurred in May 2015, only the data for May were plotted. Prior to the turbidity event (2009–2014), we found that river water levels fluctuated between 79.5 and 80.9 m, while groundwater levels exhibited variations between 38 and 43.6 m. During 2015, we observed that both the groundwater levels and river water levels experienced a significant decline. Notably, with river water levels fluctuating between 79.4 and 80.2 m, groundwater levels varied from 35.1 to 42.6 m. In 2016, the relationship between the groundwater and river water levels was lower than that observed before the turbidity event. River water levels varied from 78.7 to 79 m, while groundwater levels ranged from 33.8 to 35.4 m. Additionally, river water levels in 2016 were considerably lower than those in previous years, suggesting the possibility of reduced precipitation during that year. In 2017, the relationship was slightly below that observed before the turbidity event, with river water levels fluctuating between 79.1 and 79.9 m and

groundwater levels varying from 37.4 to 41.1 m. Furthermore, in 2018, the relationship closely resembled that observed before the turbidity event, with river water levels ranging from 79.5 to 80.1 m and groundwater levels varying from 41 to 42.4 m.

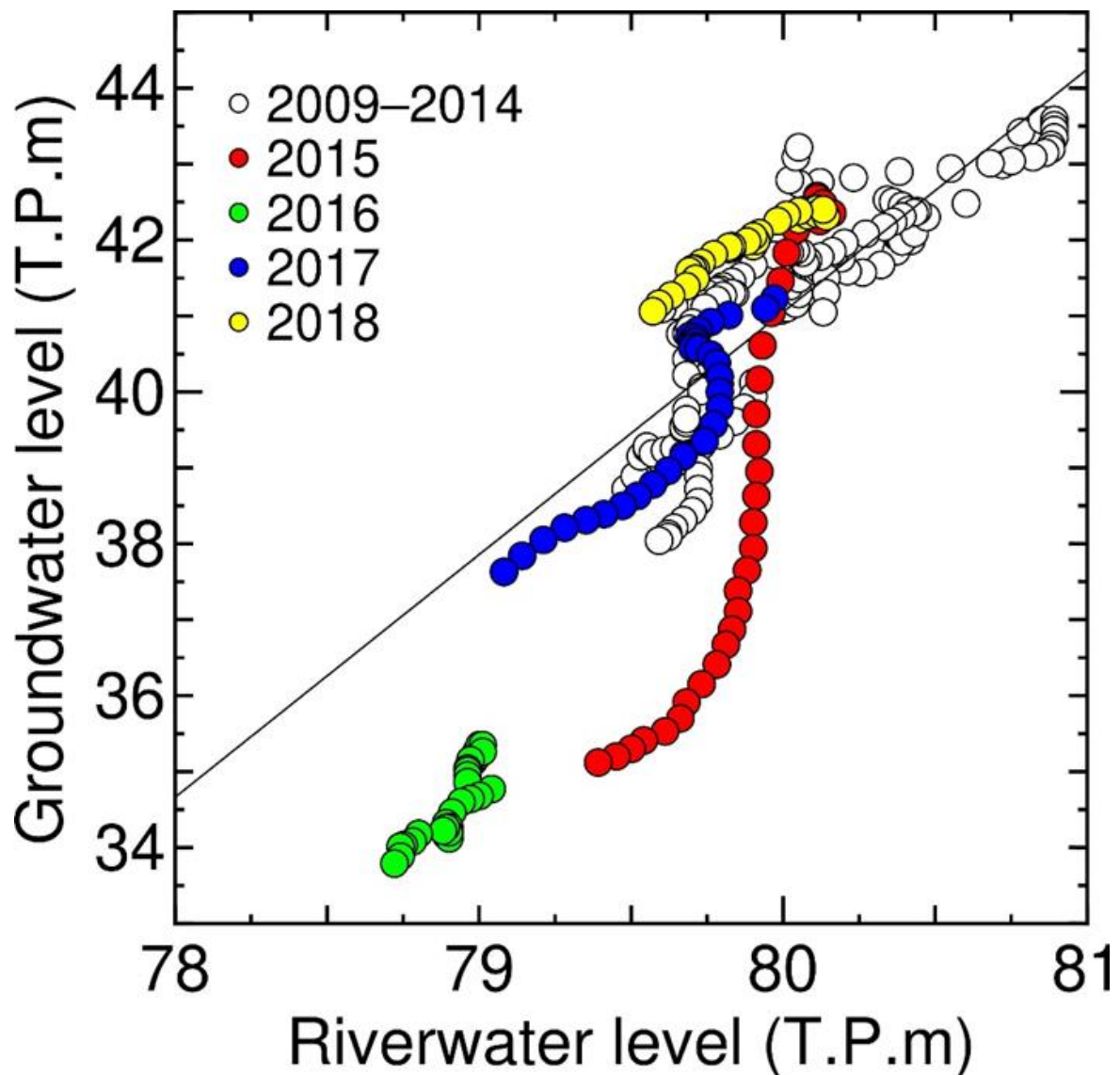


**Figure 7.** Relationship between the 14-day backward moving average of river water and groundwater levels.

#### 4.2. Seepage from River

We calculated river seepage using the water balance between river cross-sections and generated a scatterplot illustrating the relationship between seepage across the entire alluvial fan and the Tedoru River's discharge, as shown in Figure 8. With regard to the Tedoru River discharges, we evaluated the irrigation water withdrawal from the observed flow at the Nakajima monitoring station. In this figure, data from 2009 to 2014 are represented by white circles, whereas data from 2015 onwards are color coded by year. Focusing on the pre-turbidity event data from 2003 to 2014, we observed that seepages ranged from approximately 3.8 to 8.3 m<sup>3</sup>/s against river discharges of 18.7 to 40.5 m<sup>3</sup>/s. On average, before the turbidity event, approximately 24% of the Tedoru River's discharge contributed to seepage. In contrast, during the post-turbidity years, specifically in 2015, seepages ranged from 2.1 to 5.6 m<sup>3</sup>/s against river discharges of 23.3 to 24.9 m<sup>3</sup>/s. Additionally, in 2016, seepages ranged from 1.3 to 3.3 m<sup>3</sup>/s against river discharges of 22.9 to 29.8 m<sup>3</sup>/s,

accounting for approximately 4% of the river discharge. In 2017, seepage reached  $4 \text{ m}^3/\text{s}$  against a river discharge of  $29.9 \text{ m}^3/\text{s}$ . Notably, in 2018, seepage reached  $10.9 \text{ m}^3/\text{s}$  against a river discharge of  $30.9 \text{ m}^3/\text{s}$ , suggesting a return to pre-turbidity seepage levels.

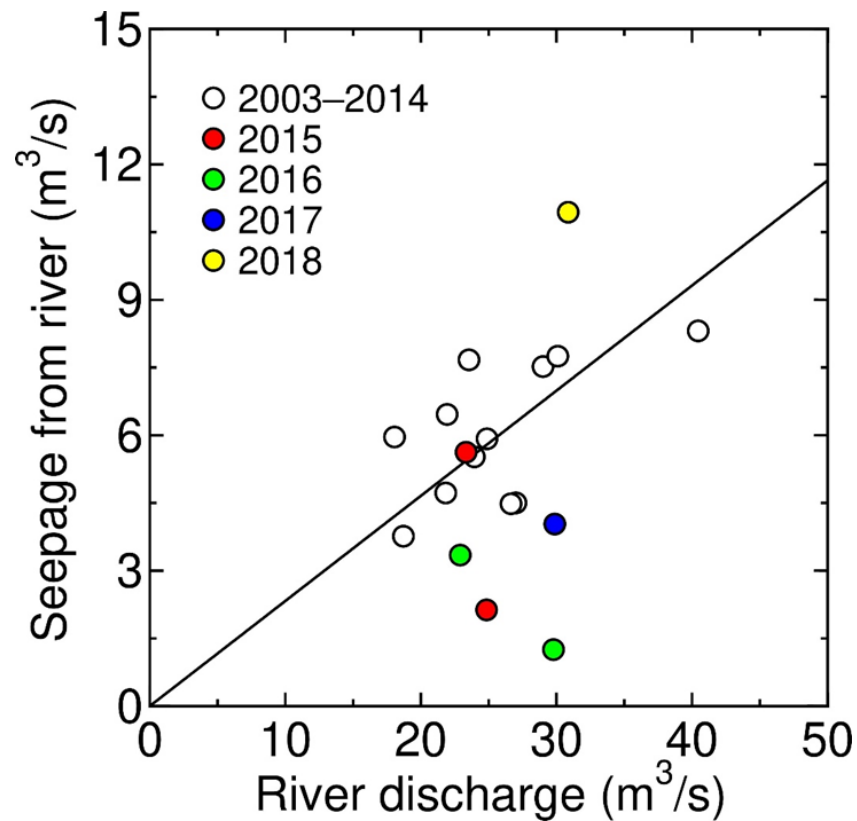


**Figure 8.** Relationship between seepages from the river and the river's discharge.

#### 4.3. Contributions

We present a comparison between the observed and computed groundwater levels for the years 2013–2014 in Figure 9. From this comparison, it is evident that the computed results closely match the observed values. The NSE was 0.76, RE was 6.0%, and PBIAS was  $-0.6\%$ . These metrics indicated the strong reproducibility of the hydrological model developed in this study. Therefore, by utilizing this model to simulate the years from 2015 onwards, we could replicate the groundwater systems that would have prevailed in the absence of turbidity events.



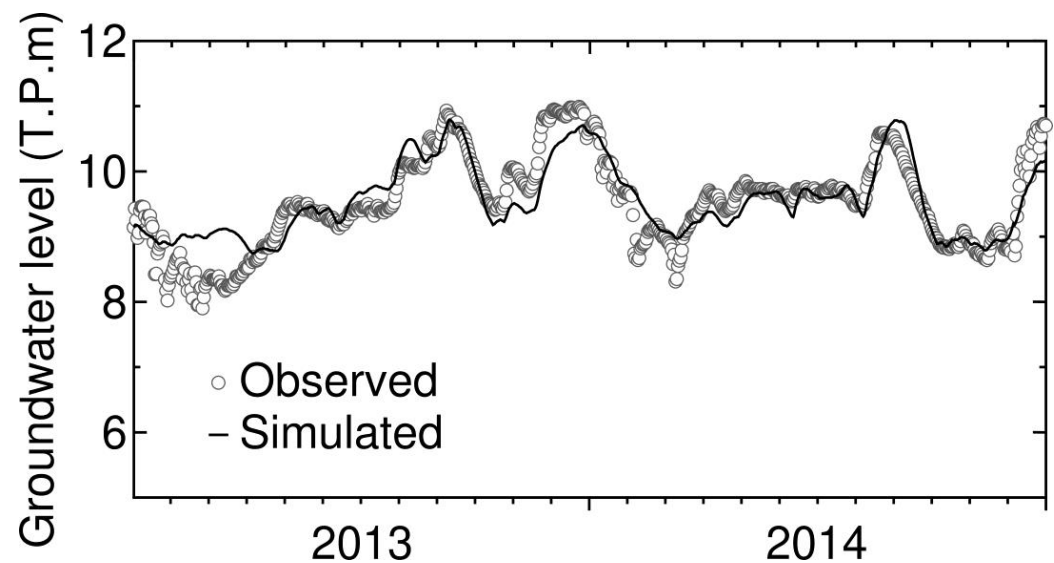


**Figure 9.** Observed and simulated groundwater levels during the calibration period.

Next, we present an analysis of the annual precipitation data from the Kanazawa Meteorological Observatory and Komatsu AMeDAS for the alluvial fan area in Table 2. Additionally, we included the annual precipitation data for the Tedoru River upper basin obtained from Kawachi and Shiramine AMeDAS in Table 2. Upon examining these data, it became evident that in the years when turbidity events occurred, specifically in 2015 and 2016, precipitation levels were considerably lower than those in 2013–2014. Specifically, the two-year average precipitation for the alluvial fan area was 2848 mm from 2013 to 2014, whereas in 2015, the precipitation dropped to 2099 mm, and in 2016, it was 2259 mm (Table 3). In the upper basin, the two-year average precipitation was 3248 mm between 2013 and 2014, 2772 mm in 2015, and 2635 mm in 2016 (Table 3). Therefore, the model input data for precipitation were adjusted on a daily basis to be 1.36 times for 2015 and 1.26 times for 2016 compared to the 2013–2014 levels. Similarly, the daily input for Nakajima flow data was adjusted to be 1.17 times for 2015 and 1.23 times for 2016. By driving the hydrological model with these data, we could reproduce groundwater levels in a scenario where turbidity did not occur, and precipitation remained at typical yearly levels.

**Table 2.** Annual precipitation for each station.

Year	Komatsu	Kanazawa	Kawachi	Shiramine
2013	3009 mm	3318 mm	3316 mm	3381 mm
2014	2430 mm	2635 mm	3351 mm	2943 mm
2015	2034 mm	2165 mm	2870 mm	2674 mm
2016	2127 mm	2391 mm	2759 mm	2512 mm
2017	2253 mm	2703 mm	3780 mm	3400 mm
2018	2694 mm	2766 mm	3548 mm	3257 mm

**Table 3.** Annual precipitation for the alluvial fan and upstream areas.

Year	Average of Komatsu and Kanazawa	Average of Kawachi and Shiramine
2-year mean (2013 and 2014)	2848 mm (100%)	3248 mm (100%)
2015	2099 mm (74%)	2772 mm (85%)
2016	2259 mm (79%)	2635 mm (81%)
2017	2478 mm (87%)	3590 mm (111%)
2018	2730 mm (96%)	3402 mm (105%)

We displayed the observed hydrograph alongside cases of no turbidity and no turbidity with normal precipitation in Figure 10. The difference between the observed values and those in case (a) represents the impact of turbidity, whereas the difference between cases (a) and (b) reflects the influence of precipitation. Comparing the observed groundwater levels with those in case (a), it is apparent that significant differences emerged from May 2015 onwards and during the first half of 2017. Moreover, when comparing cases (a) and (b), it became evident that there were consistent variations in groundwater levels throughout the entire years of 2015 and 2016. The contributions obtained are summarized in Table 4. In 2015, immediately following the turbidity event, we observed a substantial contribution of 76% from turbidity and 24% from precipitation, signifying the substantial impact of turbidity. However, in 2016, we found that turbidity contributed to 67%, whereas precipitation accounted for 33% of the groundwater level changes, indicating that lower precipitation levels had a significant influence on groundwater decline.

**Table 4.** Percentage contribution to the reduction in the groundwater level.

Year	Turbidity	Precipitation
2015	76.0%	24.0%
2016	67.2%	32.8%
2017	81.8%	18.2%

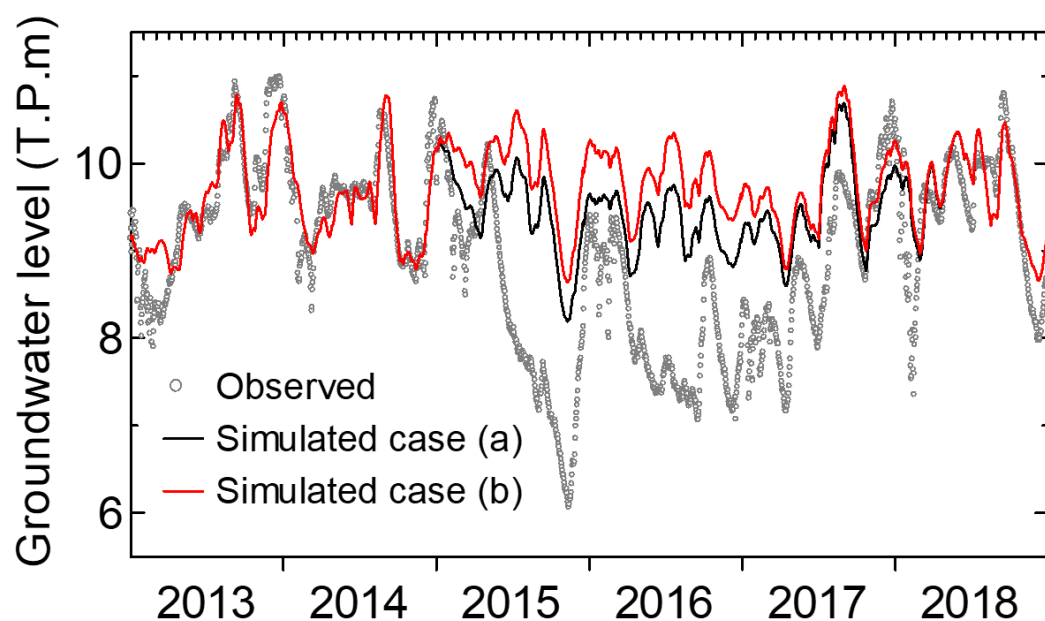


**Figure 10.** Observed and simulated groundwater levels for case (a) and (b).

## 5. Discussion

We assessed the impact of high-concentration turbidity events on the groundwater environment of the Tadori River alluvial fan, which supports local industries. Previous studies by Tanaka et al. [15,16] and Yoshioka et al. [18,19] were primarily snapshot-based studies relying on field surveys, resulting in fragmented insights. In contrast, our study investigated the continuous relationship between river water and groundwater levels (Figures 6 and 7). Leveraging the unique characteristics of this alluvial fan, which has been the subject of numerous research investigations, we also examined the changes in seepage before and after the turbidity events (Table 1 and Figure 8). Furthermore, we analyzed the impact of precipitation (Tables 2 and 3), which had not been considered in earlier studies, using hydrological model simulations (Figures 5 and 9). Consequently, we estimated the continuous contributions of turbidity and precipitation (Figure 10) and aggregated them on an annual

basis (Table 4). In 2015, turbidity accounted for 76%, while precipitation contributed to 24%; in 2016, turbidity accounted for 67%, while precipitation contributed to 33%. In essence, the first year was dominated by the influence of turbidity, while the second year saw precipitation play a substantial role in groundwater level changes.

On the other hand, in the Tedor River alluvial fan, no special engineering measures were taken to mitigate clogging. This implies that within approximately three years of the occurrence of turbidity, the groundwater levels returned to their original levels. It has been reported that the clogging was washed away by extremely high floods (e.g., Goldschneider et al. [21]; Trásy et al. [40]). Figure 6 indicates that the peak of the river water level in 2017 was larger than that in 2015 and 2016. Therefore, it is likely that clogging was eliminated in the Tedor River alluvial fan by a similar mechanism. However, our study employed a concentrated hydrological model that did not account for the spatial variability in the subsurface flow. Therefore, it was not possible to elucidate where in the river permeability decreased. To achieve more precise groundwater management, it is crucial to elucidate the spatial variability of the subsurface flow. These aspects are areas for future research.

## 6. Conclusions

In the downstream areas of the Tedor River Basin, an alluvial fan is spread out, and paddy field agriculture is the predominant activity in these areas. In these regions, river infiltration and seepage from rice fields are valuable sources of groundwater. However, the occurrence of high-concentration turbidity resulting from large-scale landslides in the upper reaches of the basin has led to a rapid drop in groundwater levels in these alluvial fans. It is essential to determine when groundwater recharge from the river and rice fields begins to recover and assess the magnitude of their contributions to sustainable groundwater management.

Through the analysis of the relationship between river water levels and groundwater levels, it was determined that by 2018, the conditions had reverted to those observed before the turbidity events. Similar results were obtained for the river seepage measured using the water balance of the river flows. Furthermore, by constructing a hydrological model for the alluvial fan area and examining the contributions of turbidity and precipitation, it was revealed that in 2015, turbidity contributed to 76% of the groundwater level changes, whereas precipitation accounted for 24%. In contrast, for the year 2016, turbidity contributed to 67%, while precipitation contributed to 33%. The first year was characterized by a significant influence of turbidity, whereas the second year showed that precipitation also played a substantial role in groundwater level fluctuations. The modeling approach used in this study can be applied to other alluvial fans and plains worldwide to evaluate riverbed clogging. The results of this approach will also help in understanding the interaction between river water and groundwater, and in considering sustainable groundwater resource management.

**Author Contributions:** Conceptualization, Y.F. and K.T.; methodology, K.O.; software K.O.; formal analysis, Y.F. and K.O.; investigation, Y.F., K.O. and S.C.; resources, K.T.; data curation, Y.F.; writing—original draft preparation, Y.F.; writing—review and editing, E.I.; visualization, K.O.; supervision, E.I.; project administration, Y.F.; funding acquisition, Y.F. All authors have read and agreed to the published version of the manuscript.

**Funding:** This research was financially supported by the Japan Society for the Promotion of Science (JSPS) KAKENHI Grant Number 22H02461, the Japan Geographic Data Center, and the River Fund of the River Foundation, Japan.

**Data Availability Statement:** Groundwater level data within the fan were provided by Ishikawa Prefecture. Data on river water levels were provided by the Ministry of Land, Infrastructure, Transport and Tourism. AMEDAS data were collected from the Japan Meteorological Agency website (<https://www.data.jma.go.jp/stats/etrn/index.php> accessed on 1 April 2024).

**Acknowledgments:** We would like to express our sincere thanks to Hokkoku Shimbun for their helpful support during the field surveys.

**Conflicts of Interest:** Author Kento Otani (K.T.) was employed by the Kokusai Kogyo Company, Limited. The remaining authors declare that the research was conducted in the absence of any commercial or financial relationships that could be construed as potential conflicts of interest.

## References

1. Ministry of Land, Infrastructure, Transport and Tourism. Current State of Water Resources in Japan 2022. Available online: [https://www.mlit.go.jp/mizukokudo/mizsei/mizukokudo\\_mizsei\\_tk2\\_000039.html](https://www.mlit.go.jp/mizukokudo/mizsei/mizukokudo_mizsei_tk2_000039.html) (accessed on 9 April 2024).
2. Liu, Y.; Yamanaka, T.; Zhou, X.; Tian, F.; Ma, W. Combined use of tracer approach and numerical simulation to estimate groundwater recharge in an alluvial aquifer system: A case study of Nasunogahara area, central Japan. *J. Hydrol.* **2014**, *519*, 833–847. [\[CrossRef\]](#)
3. Tsuchihara, T.; Shirahata, K.; Ishida, S.; Yoshimoto, S. Application of a Self-organizing map of isotopic and chemical data for the identification of groundwater recharge sources in Nasunogahara Alluvial Fan, Japan. *Water* **2020**, *12*, 278. [\[CrossRef\]](#)
4. Yu, H.L.; Chu, H.J. Understanding space–time patterns of groundwater system by empirical orthogonal functions: A case study in the Choshui River alluvial fan, Taiwan. *J. Hydrol.* **2010**, *381*, 239–247. [\[CrossRef\]](#)
5. Noto, F.; Maruyama, T.; Hayase, Y.; Takimoto, H.; Nakamura, K. Evaluation of water resources by snow storage using water balance and tank model method in the Tedor River basin of Japan. *Paddy Water Environ.* **2013**, *11*, 113–121. [\[CrossRef\]](#)
6. Noto, F.; Maruyama, T.; Yoshida, M.; Hayase, Y.; Takimoto, H.; Nakamura, K. Prediction of water resources as snow storage under climate change in the Tedor River basin of Japan. *Paddy Water Environ.* **2013**, *11*, 463–471. [\[CrossRef\]](#)
7. Maruyama, T.; Takimoto, H.; Ogura, A.; Yoshida, M. Analysis of snowpack accumulation and the melting process of wet snow using a heat balance approach that emphasizes the role of underground heat flux. *J. Hydrol.* **2015**, *522*, 369–381. [\[CrossRef\]](#)
8. Fujihara, Y.; Takase, K.; Chono, S.; Ichion, E.; Ogura, A.; Tanaka, K. Influence of topography and forest characteristics on snow distributions in a forested catchment. *J. Hydrol.* **2017**, *546*, 289–298. [\[CrossRef\]](#)
9. Iwasaki, Y.; Ozaki, M.; Nakamura, K.; Horino, H.; Kawashima, S. Relationship between increment of groundwater level at the beginning of irrigation period and paddy filed area in the Tedor River Alluvial Fan Area, Japan. *Paddy Water Environ.* **2013**, *11*, 551–558. [\[CrossRef\]](#)
10. Yoshioka, Y.; Nakamura, K.; Horino, H.; Nakano, T.; Shin, K.C.; Kawashima, S. Evaluation of groundwater qualities in a paddy-dominated alluvial fan. *Water Supply* **2015**, *15*, 1236–1243. [\[CrossRef\]](#)
11. Yoshioka, I.Y.; Nakamura, K.; Nakano, T.; Horino, H.; Shin, K.C.; Hashimoto, S.; Kawashima, S. Multiple-indicator study of groundwater flow and chemistry and the impacts of river and paddy water on groundwater in the alluvial fan of the Tedor River, Japan. *Hydrol. Process.* **2016**, *30*, 2804–2816. [\[CrossRef\]](#)
12. Maruyama, T.; Noto, F.; Yoshida, M.; Horino, H.; Nakamura, K. Analysis of water balance in the Tedor river alluvial fan areas of Japan: Focused on quantitative analysis of groundwater recharge from river and ground surface, especially paddy fields. *Paddy Water Environ.* **2014**, *12*, 163–171. [\[CrossRef\]](#)
13. Yoshioka, Y.; Nakamura, K.; Horino, H.; Kawashima, S. Numerical assessments of the impacts of climate change on regional groundwater systems in a paddy-dominated alluvial fan. *Paddy Water Environ.* **2016**, *14*, 93–103. [\[CrossRef\]](#)
14. Yanai, S. Characteristics of a landslide occurred in May 2015 in Mt. Hakusan and its influence on downstream system. In Proceedings of the Symposium Proceedings of the INTERPRAENENT 2018 in the Pacific Rim, Toyama, Japan, 1–4 October 2018; pp. 124–131.
15. Tanaka, K.; Segawa, M.; Fujihara, Y.; Takase, K.; Maruyama, T.; Chono, S. High-turbidity water from landslides affects groundwater recharge of paddy fields in the Tedor River alluvial fan. *J. Jpn. Soc. Hydrol. Water Resour.* **2017**, *30*, 173–180. (In Japanese with English Abstract) [\[CrossRef\]](#)
16. Tanaka, K.; Segawa, M.; Fujihara, Y.; Takase, K.; Maruyama, T.; Chono, S. Influence of high-turbidity water on paddy percolation and riverbed seepage in an alluvial fan. *Trans. Jpn. Soc. Irrig. Drain. Rural. Eng.* **2018**, *306*, I\_47–I\_54. (In Japanese with English Abstract) [\[CrossRef\]](#)
17. Nishizono, Y.; Ichion, E.; Ueda, T.; Kitamura, K.; Yamabuki, H. Evaluation of canal rehabilitation works executed with attention to a habitat of the freshwater type of nine-spined stickleback. In Proceedings of the 21st annual congress of Japan Rainwater Catchment Systems Association, Matsue, Japan, 2–3 November 2013; pp. 49–54.
18. Yoshioka, Y.; Ito, M.; Nakamura, K.; Takimoto, H.; Tsuchihara, T. Assessing the river water–Groundwater interaction and sources of groundwater recharge based on oxygen and hydrogen isotope analyses in the Tedor River Alluvial Fan. *J. Groundw. Hydrol.* **2018**, *60*, 205–221. (In Japanese with English Abstract) [\[CrossRef\]](#)
19. Yoshioka, Y.; Nakamura, K.; Takimoto, H.; Sakurai, S.; Nakagiri, T.; Horino, H.; Tsuchihara, T. Multiple-indicator study of the response of groundwater recharge sources to highly turbid river water after a landslide in the Tedor River alluvial fan, Japan. *Hydrol. Process.* **2020**, *34*, 3539–3554. [\[CrossRef\]](#)
20. Hokuriku Regional Agricultural Administration Office. *Hydraulic Geology and Groundwater in Ishikawa Prefecture*; Hokuriku Regional Agricultural Administration Office: Kanazawa, Japan, 1977. (In Japanese)
21. Goldschneider, A.A.; Haralampides, K.A.; MacQuarrie, K.T.B. River sediment and flow characteristics near a bank filtration water supply: Implications for riverbed clogging. *J. Hydrol.* **2007**, *344*, 55–69. [\[CrossRef\]](#)



22. Lamontagne, S.; Taylor, A.R.; Cook, P.G.; Crosbie, R.S.; Brownbill, R.; Williams, R.M.; Brunner, P. Field assessment of surface water-groundwater connectivity in a semi-arid river basin (Murray-Darling, Australia). *Hydrol. Process.* **2014**, *28*, 1561–1572. [\[CrossRef\]](#)
23. Dubuis, R.; De Cesare, G. The clogging of riverbeds: A review of the physical processes. *Earth-Sci. Rev.* **2023**, *239*, 104374. [\[CrossRef\]](#)
24. Harte, P.T.; Kiah, R.G. Measured river leakages using conventional streamflow techniques: The case of Souhegan River, New Hampshire, USA. *Hydrogeol. J.* **2009**, *17*, 409–424. [\[CrossRef\]](#)
25. Kinzli, K.D.; Martinez, M.; Oad, R.; Prior, A.; Gensler, D. Using an ADCP to determine canal seepage loss in an irrigation district. *Agric. Water Manag.* **2010**, *97*, 801–810. [\[CrossRef\]](#)
26. Martin, C.A.; Gates, T.K. Uncertainty of canal seepage losses estimated using flowing water balance with acoustic Doppler devices. *J. Hydrol.* **2014**, *517*, 746–761. [\[CrossRef\]](#)
27. Abdu, H.; Robinson, D.A.; Seyfried, M.; Jones, S.B. Geophysical imaging of watershed subsurface patterns and prediction of soil texture and water holding capacity. *Water Resour. Res.* **2008**, *44*, W00D18. [\[CrossRef\]](#)
28. Thakur, J.K. Hydrogeological modeling for improving groundwater monitoring network and strategies. *Appl. Water Sci.* **2017**, *7*, 3223–3240. [\[CrossRef\]](#)
29. Siena, M.; Riva, M. Impact of geostatistical reconstruction approaches on model calibration for flow in highly heterogeneous aquifers. *Stoch. Environ. Res. Risk Assess.* **2020**, *34*, 1591–1606. [\[CrossRef\]](#)
30. Takase, K.; Fujihara, Y. Evaluation of the effects of irrigation water on groundwater budget by a hydrologic model. *Paddy Water Environ.* **2019**, *17*, 439–446. [\[CrossRef\]](#)
31. Takase, K.; Fujihara, Y. Analysis of influences of high-turbidity river water on groundwater level in the Tedor River alluvial fan using a lumped hydrologic model. *Trans. Jpn. Soc. Irrig. Drain. Rural. Eng.* **2022**, *314*, I\_167–I\_173, (In Japanese with English Abstract). [\[CrossRef\]](#)
32. Fujihara, Y.; Oda, M.; Horikawa, N.; Ogura, C. Hydrologic analysis of rainfed rice areas using a simple semi-distributed water balance model. *Water Resour. Manag.* **2011**, *25*, 2061–2080. [\[CrossRef\]](#)
33. Hang, N.T.T.; Chikamori, H. Comparison of efficiency between differential evolution and evolution strategy: Application of the LST model to the Be River catchment in Vietnam. *Paddy Water Environ.* **2017**, *15*, 797–808. [\[CrossRef\]](#)
34. Duan, Q.; Sorooshian, S.; Gupta, V.K. Effective and efficient global optimization for conceptual rainfall-runoff models. *Water Resour. Res.* **1992**, *28*, 1015–1031. [\[CrossRef\]](#)
35. Duan, Q.; Sorooshian, S.; Gupta, V.K. Optimal use of the SCE-UA global optimization method for calibrating watershed models. *J. Hydrol.* **1994**, *158*, 265–284. [\[CrossRef\]](#)
36. Gupta, H.V.; Sorooshian, S.; Yapo, P.O. Status of automatic calibration for hydrologic models: Comparison with multilevel expert calibration. *J. Hydrol. Eng.* **1999**, *4*, 135–143. [\[CrossRef\]](#)
37. De Vos, N.J.; Rientjes, T.H.M. Multiobjective training of artificial neural networks for rainfall-runoff modeling. *Water Resour. Res.* **2008**, *44*, W08434. [\[CrossRef\]](#)
38. Shi, P.; Chen, C.; Srinivasan, R.; Zhang, X.; Cai, T.; Fang, X.; Qu, S.; Chen, X.; Li, Q. Evaluating the SWAT Model for hydrological modeling in the Xixian watershed and a comparison with the XAJ Model. *Water Resour. Manag.* **2011**, *25*, 2595–2612. [\[CrossRef\]](#)
39. Schiavo, M. The role of different sources of uncertainty on the stochastic quantification of subsurface discharges in heterogeneous aquifers. *J. Hydrol.* **2023**, *617*, 128930. [\[CrossRef\]](#)
40. Trásy, B.; Kovács, J.; Hatvani, I.G.; Havril, T.; Németh, T.; Scharek, P.; Szabó, C. Assessment of the interaction between surface- and groundwater after the diversion of the inner delta of the River Danube (Hungary) using multivariate statistics. *Anthropocene* **2018**, *22*, 51–65. [\[CrossRef\]](#)

**Disclaimer/Publisher’s Note:** The statements, opinions and data contained in all publications are solely those of the individual author(s) and contributor(s) and not of MDPI and/or the editor(s). MDPI and/or the editor(s) disclaim responsibility for any injury to people or property resulting from any ideas, methods, instructions or products referred to in the content.